PANI-derived polymer/Al_2O_3 nanocomposites: Synthesis, characterization and electrochemical studies

A Bekhoukh [1], M. Mekhloufi [1], R. Berenguer [2], A. Benyoucef [1 *], E. Morallon [2]

[1]*Laboratoire de Chimie Organique, Macromoléculaire et des Matériaux, Université de Mustapha Stambouli Mascara. Bp 763 Mascara 29000 (Algeria)*

[2]*Departamento de Química Física e Instituto Universitario de Materiales, Universidad de Alicante, Apartado 99, E-03080 Alicante (Spain)*

[*]Corresponding author

e-mail: abdelghani@ua.es

benyoucef.abdelghani@www.univ-mascara.dz

Telf.: (+213)771707184

Fax: (+213)45930118

Abstract

This paper presents the physicochemical, conductive, and electrochemical properties of different polyaniline(PANI)-derived polymer/Al_2O_3 nanocomposites synthesized by chemical oxidation polymerization method carried out in two-stages. First, activation of the surface of the Al_2O_3 nanoparticles by hydrochloric acid. Second, polymerization of 2-chloroaniline (2ClANI), aniline (ANI) and the co-polymer (2ClANI-ANI) in the presence of Al_2O_3 using ammonium persulfate as oxidant in aqueous hydrochloric acid. XRD and TEM results reveal the growth of the polymers on Al_2O_3 nanoparticles and the formation of PANI-derived polymer/Al_2O_3 nanocomposites. FTIR and UV-Vis show a systematic shifting of the characteristic bands of the polymers with the presence of Al_2O_3 nanoparticles. Moreover, these nanoparticles enhance the thermal stability of the polymers, as found by thermogravimetric analysis (TGA). Although the incorporation of Al_2O_3 nanoparticles reduces the electric conductivity of the polymers, the resulting nanocomposites still keep high conductivities, ranging between $0.3x10^{-2}$ to $9.2x10^{-2}$ S cm^{-1}. As a result, the polymer/Al_2O_3 nanocomposites exhibit a good voltammetric response. All these synergetic features of the nanocomposites are assigned to the effective interaction of the polymers and Al_2O_3 particles at nano-scale.

Keywords: Polyaniline; 2-Chloroaniline; Aluminum oxide; Nanocomposite; Electrochemical properties.

Introduction

Conducting polymers have been extensively studied for various applications [1, 2]. Among them, polyaniline is one of the most promising due to its unique properties: easy synthesis in aqueous media, excellent ambient stability and simplicity in doping [3, 4]. The doping level can be controlled through a non-redox acid doping/base dedoping process [5]. By changing the doping level, the conductivity of polyaniline can be modified to suit specific applications. On the other hand, unlike acids and bases, oxidizing and reductant chemicals can change the conductivity of polyaniline by changing its inherent oxidation state. The conductivity of polyaniline depends on both the oxidation state of the main polymer chain and the degree of protonation on imine sites [6].

Furthermore, functional additives incorporated into the polymer matrix, such as metals, metal oxides and enzymes can also affect the characteristics of polyaniline [7]. Such a high versatility for tailoring its conductivity has made polyaniline an attractive material for a broad scope of design and development of smart sensors [7].

Magnetic nanostructures have been intensively studied due to the fact that they can be used in a wide range of applications such as clinical diagnosis, mineral separation, magnetic storage devices, absorption of microwave radiation, magneto-optic materials, microwave filters and hybrid materials [8-10].

The high purity metal oxides nanoparticles were synthesized as yet by variety methods such as precipitation, hot-air spray pyrolysis, sol-gel, hydrothermal and sonochemical [9-15].

Regarding these additives, the development of inorganic/polymer nanocomposite materials has received significant interest due to the wide range of potential applications in optoelectronic devices [16, 17] and electromagnetic interference shielding [18]. These

composites have been prepared by different techniques and they exhibit a synergetic behavior between the polymer and the inorganic material [8-12, 45,46, 19]. Since at nano-scale the surface to volume ratio is large, the nano-sized inorganic material is expected to largely modify the thermal, electrical, optical and dielectric properties of the polymer.

In addition, the different properties of components provide the nanocomposites with preferential capabilities for specific applications. For example, alumina has a large surface area, adsorption capacity, and shows good wear resistance [20, 21], so it is commonly used as catalyst, catalyst support, filter, and filler for polymers to improve mechanical properties [22, 23]. At least, seven different transitional aluminas have been reported and Al_2O_3 nanoparticle is perhaps, the most important one for its industrial applications [13,15, 24, 45].

In the present investigation, different polymers and copolymers based on aniline and chloroaniline and their composites with Al_2O_3 were prepared by in situ chemical oxidative polymerization using hydrochloric acid as dopant and ammonium persulphate as an oxidant. The resulting samples were characterized by FTIR, UV and XRD. The thermal properties of the materials were studied by TGA analysis and the electrical conductivities were measured by using the four-point probe method. The electrochemical behavior of the nanocomposites has been analyzed by cyclic voltammetry.

Experimental

Materials

The monomer aniline (ANI) (Aldrich) was distilled under vacuum prior to use, whereas 2-Chloroaniline (2ClAni) (Aldrich) was used as received. Perchloric acid and hydrochloric acid (Merck) were suprapur quality and all the solutions were freshly prepared with distilled-deionised water obtained from an Elga Labwater Purelab Ultra system.

Aluminum oxide nanoparticles (Al_2O_3) (99%) was purchased from Sigma-Aldrich. Ammonium persulfate (APS) and ammonia solution (NH_4OH) were of analytical purity and used without further purification.

Chemical synthesis of nanocomposites

The homopolymers of chloroaniline (poly(2ClAni)) and aniline (PANI), the copolymer of aniline with chloroaniline (poly(2ClAni-co-Ani)), and their corresponding nanocomposites with Al_2O_3: poly(2ClAni)/Al_2O_3, poly(2ClAni-co-Ani)/Al_2O_3 and PANI/Al_2O_3, respectively, were synthesized by the in-situ chemical oxidative polymerization method [25]. This polymerization procedure is schematized in Fig. 1 [26]. Firstly, a certain amount of Al_2O_3 nanoparticles was dispersed in HCl (0.1 M) under simultaneous mechanical stirring and sonication for 1 h, to activate the surface of Al_2O_3. Then, an equimolar solution (0.25 mol) of the monomer (2ClAni or/and Ani) and hydrochloric acid was prepared and kept at 5 ºC. 0.5 g of activated Al_2O_3 nanoparticles were added to the above solution and subsequently submitted to vigorous stirring (30 min) to keep the activated Al_2O_3 suspended in the solution. Afterwards, a pre-cooled solution of APS (1 M) was added drop-wise under constant stirring. The reaction was allowed to process at about 5 °C for 24 h. Since the surface charge of Al_2O_3 is positive in acidic conditions, an amount of Cl^- is adsorbed on the surface of nanoparticles to compensate the positive charges. In the same acidic conditions, the monomers (2-ClAni and/or Ani) are converted to cationic anilinium ions. This leads to electrostatic interactions between the adsorbed anions and cationic anilinium ions. The precipitates were filtered and washed several times with distilled water and acetone until the filtrate was colorless. The final products were maintained in 50 mL of 1 M NH_4OH at room temperature while magnetically stirring for 2 h. The precipitate product was collected by

filtering and after washing with deionized water and drying under vacuum at 60°C for 24 h [25, 27].

Physicochemical Characterization

The X-ray diffraction of the powder nanocomposites were obtained using a Bruker CCD-Apex equipment with a X-ray generator (Cu $K\alpha$ and Ni filter) operated at 40 kV and 40 mA. A Hitachi U-3000 spectrophotometer was used for recording the UV-Vis spectra. The homopolymers and co-polymers were dissolved in N-methyl-2-pyrrolidone (NMP). Fourier transform infrared (FT-IR) spectroscopy was recorded using a Bruker Alpha.

For Transmission Electron Microscopy (TEM) observations, the samples were dispersed in ethanol and supported on TEM grids. The images were collected using a JEOL (JEM-2010) microscope, working at an operation voltage of 200 kV. The TEM is coupled with Energy Dispersive X-ray Spectroscopy (EDS) for the elucidation of chemical composition of the samples.

The thermogravimetric analysis (TGA) was performed with a Du Pont thermogravimetric analyzer at a heating rate of 20 °C/min under nitrogen. About 10 mg of sample was heated up to 900°C.

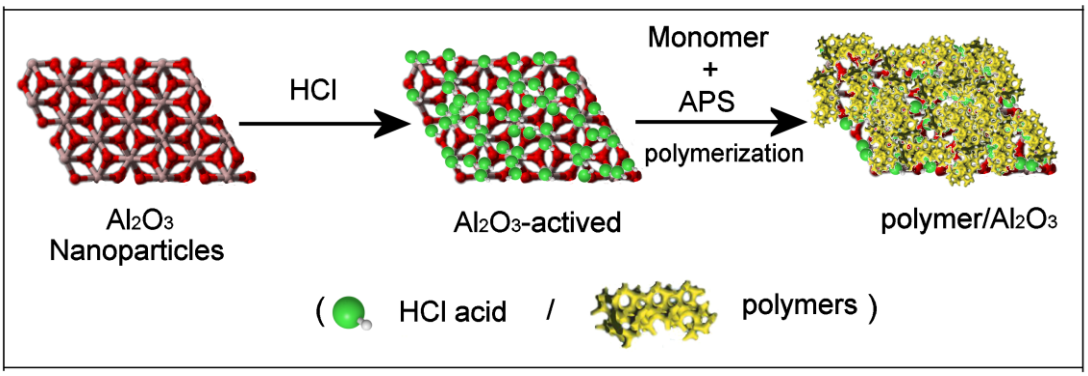

Fig. 1. Scheme of polymer/Al_2O_3 nanocomposites preparation.

Electrochemical characterization

The electrochemical behavior of the nanocomposites and the polymers was studied by cyclic voltammetry. The nanocomposite was first dissolved in N-methyl-2-pyrrolidone (NMP) in which the polymers are soluble; then the dissolved polymers are extracted from the nanocomposites [25]. Then, a drop of resulting solution was placed on the glassy carbon electrode (0.07 cm^2 of geometrical area) and dried in air under an infrared lamp to remove the solvent. The electrochemical measurements were carried out using a conventional three-electrodes cell. The counter and reference electrodes were a platinum wire and a reversible hydrogen electrode (RHE) immersed in the supporting electrolyte, respectively. The electrolyte used was 1 M $HClO_4$ and all experiments performed at 50 mV s^{-1}.

Electrical conductivity measurements

Electrical conductivity measurements were carried out by using a Lucas Lab resistivity equipment of four probes in-line. The samples were dried under vacuum for 24 h and shaped into pellets (0.013 m diameter) by using a FTIR mold and applying a pressure of 7.4 10^8 Pa.

Results and discussion

Fourier-transform infrared spectra (FTIR)

The IR spectra of poly(2ClAni), poly(2ClAni-co-Ani), Al_2O_3 nanoparticles and poly(2ClAni)/Al_2O_3, poly(2ClAni-co-Ani)/Al_2O_3 and PANI/Al_2O_3 nanocomposites are shown in Fig. 2. The IR characteristic bands of all samples are tabulated in Table 1.

The –N–H stretching bands of pure polymers appear at around 3231 cm^{-1} [27]. The characteristic bands due to quinoid and benzenoid rings appear around 1563 cm^{-1} and 1495 cm^{-1}, respectively [27, 28]. In the case of poly(2ClAni), the band at 1297 cm^{-1} is due to

aromatic –C–N– stretching vibration, whereas that at around 1174 cm^{-1} corresponds to charged species (B-N^{+}H-B/Q=N^{+}H-B) present in the emeraldine salt structure [28]. The bands at 815 cm^{-1} have been assigned to –C–H out of plane bending vibration of 1, 2, 4 tri-substituted aromatic rings [29]. The band at 615 cm^{-1} is attributed to the chlorine atom attached to the phenyl ring [29]. All the above bands confirm the formation of poly(2-ClAni). The ratio of the area of benzenoid and quinonoid band is 1:3 which indicates the formation of emeraldine salt structure [30].

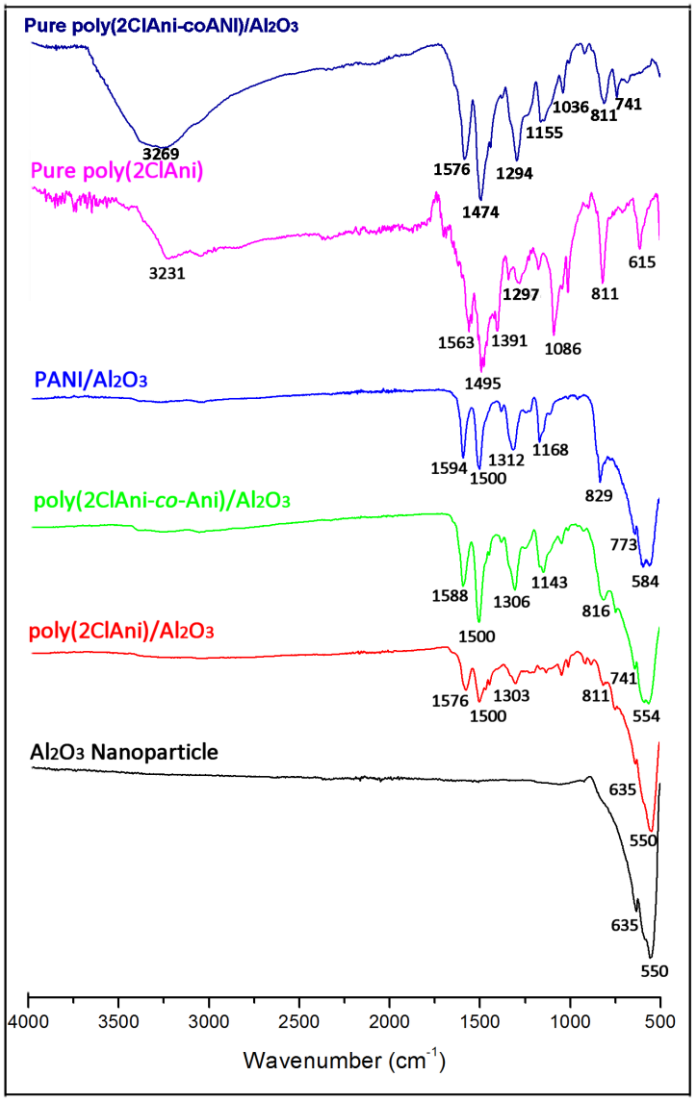

Fig. 2. FT-IR adsorption spectra of Al_2O_3 nanoparticle, poly(2ClAni), poly(2ClAni-co-Ani), poly(2ClAni)/Al_2O_3, poly(2ClAni-co-Ani)/Al_2O_3 and PANI/Al_2O_3 nanocomposites.

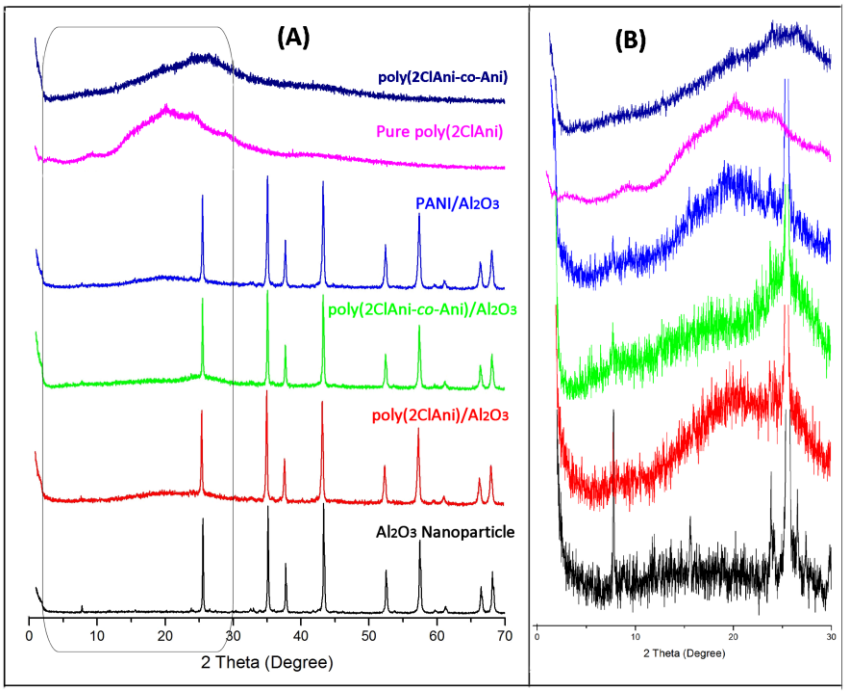

Fig. 3. XRD diffraction patterns of poly(2ClAni), poly(2ClAni-co-Ani), Al_2O_3 nanoparticule, poly(2ClAni)/Al_2O_3, poly(2ClAni-co-Ani)/Al_2O_3 and PANI/Al_2O_3 nanocomposites : (A) Experimental result between 2-70 (2θ) ; (B) zoom-in inset for the angles 2–30 (2θ).

In the case of poly(2ClAni-co-ANI), these bands are also observed and the specific positions are included in Table 1.

The IR spectrum of Al_2O_3 nanoparticles is represented by two clear bands located at 550 cm^{-1} and 635 cm^{-1}. These bands have been assigned to condensed AlO_6 octahedral, i.e. the building units in alumina structure, and are considered a fingerprint of this material [31].

The presence of Al_2O_3 bands in the IR spectrum of poly(2ClAni)/Al_2O_3 and poly(2ClAni-co-ANI)/Al_2O_3 nanocomposites confirms the incorporation of the nanoparticles into the polymer matrix. Although with lower intensity, the band related to charged species at 1174 cm^{-1} and 1155 cm^{-1} points out that the polymers in the poly(2ClAni)/Al_2O_3 and poly(2ClAni-co-ANI)/Al_2O_3 nanocomposites are in the emeraldine base form. Nevertheless, the bands characteristic of -N–H and benzenoid and quinonoid rings are all shifted in the

polymer/Al_2O_3 blend. These results suggest that the Al_2O_3 nanoparticles effectively interact with the polymer chains, affecting their vibrational modes and, therefore, their structural and physicochemical properties.

X-ray diffraction (XRD) studies

The crystalline structure of the different blends was characterized by XRD measurements. As shown in Fig. 3a, the diffraction peaks at 2θ = 25.55°, 35.14°, 37.74°, 43.38°, 52.51° and 57.53° are in good agreement with the standard profile of Al_2O_3, corresponding to the crystal planes of (012), (104), (110), (113), (024) and (116) (JCPDS card No. 87-0245), respectively. However, some obvious changes are observed on the spectra of these blends at low bragg angles, with the appearance of a broad peak between 10 to 30 º (Fig. 3b) after polymerization. These broad peaks are characteristic of amorphous structures, so they are attributed to the presence of polymers, confirming the formation of polymer/Al_2O_3 nanocomposites by the in-situ polymerization approach [32].

Electrical conductivity characterization

The electrical conductivity of poly(2ClAni), poly(2ClAni-co-Ani), PANI, poly(2ClAni)/Al_2O_3, poly(2ClAni-co-ANI)/Al_2O_3 and PANI/Al_2O_3 nanocomposites was found to vary between $14.8x10^{-2}$ and $2.52x10^{-3}$ $S{\cdot}cm^{-1}$ (Table 2). Seanor et al. [33] observed that the conductivity range for semi-conductive materials is known to be $10^{-7} - 10^{2}$ $S.cm^{-1}$. Conductivities of most doped conducting polymers lie approximately in this region [34]. The addition of Al_2O_3 nanoparticles in the different polymer matrices causes a conductivity decrease with respect to the pure polymers. This result is expected, because alumina is a non-conducting material. Polymers like (poly(2ClAni), poly(2ClAni-co-ANI) or PANI have a conjugated system which enables easy transportation of electrons. In this sense, the decreased

conductivity of nanocomposites suggests that Al_2O_3 nanoparticles interrupt and/or hindrance the electron transportation path of polymers, probably by decreasing the length of polymer chains. Once again, these results are indicative of a strong interaction at nano-interphase between the polymer chains and the Al_2O_3 nanoparticles.

UV-Vis spectroscopy

The UV-visible spectra of PANI/Al_2O_3, poly(2ClAni)/Al_2O_3, poly(2ClAni-co-ANI)/Al_2O_3 nanocomposite and Al_2O_3 nanoparticles are shown in Fig. 4. Several absorption bands are observed, the first one between 314 and 372 nm is assigned to the π-π* transitionand it is related to the extended conjugation between adjacent rings in polymeric chain. Considering that the polymers studied are less conjugated than PANI, it is reasonable that this band occurs at lower wavelength (in PANI appears at 326 nm) [26, 27]. The second band between 539 and 616 nm, in the visible zone, is assigned to the transition of the exciton of the quinone and is related to the hopping electronic intra and interchain [35, 36]. The maximun of this band depends on the polymer oxidation, and also shows a hypsocromic shift from 630 nm (in the case of PANI [36]) to 615 nm for the poly(2ClAni) and poly(2ClAni-co-ANI). This effect can be due to steric hindrace of chlorine in the PANI structure which disturb the coplanarity of the π system avoiding electron hopping, decreasing the conductivity. Finally, the intensity of this second band decreases drastically for the nanocomposites in comparison to the polymers and also are shifted to lower wavelength, this result are in agreement with the decrease in conductivity of the nanocomposites.

Thermogravimetric analysis (TGA)

The thermal stability of the different materials was evaluated by thermogravimetry. Fig. 5. shows the TG of poly(2ClAni), poly(2ClAni-co-ANI), PANI/Al_2O_3,

poly(2ClAni)/Al_2O_3 and poly(2ClAni-co-ANI)/Al_2O_3 nanocomposites. The curve of pure Al_2O_3 nanoparticles only shows a small weight loss, occurring below 400°C, that can be ascribed to the elimination of water and ethanol and the partial dehydroxylation of the Al_2O_3 nanoparticles [37]. In fact, the influence of the inorganic nanoparticles on the thermal stability of polymer/Al_2O_3 nanocomposites is very complex; which is related to many factors; such as the synthetic method; type of inorganic nanoparticles; structure of composites; the interaction between two components; and so on [38].

At temperatures lower than 130 °C, poly(2ClAni) presents a weight loss of 1.4 wt% , attributed to the volatilization of water absorbed by the polymer in the form of moisture [39]. In the temperature range of 130-210 ºC, poly(2ClAni) loses about 3.1 wt% of its weight and losing in total about 54.5 wt% between 210-550 ºC.

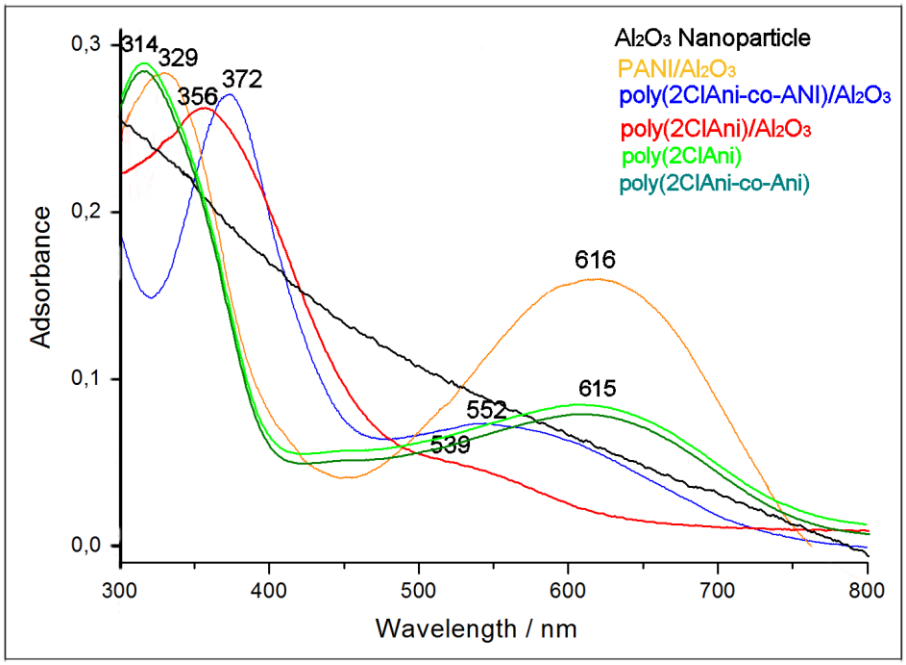

Fig. 4. UV-vis spectra of Al_2O_3 nanoparticule, poly(2ClAni)/Al_2O_3, poly(2ClAni-co-Ani)/Al_2O_3 and PANI/Al_2O_3 nanocomposites.

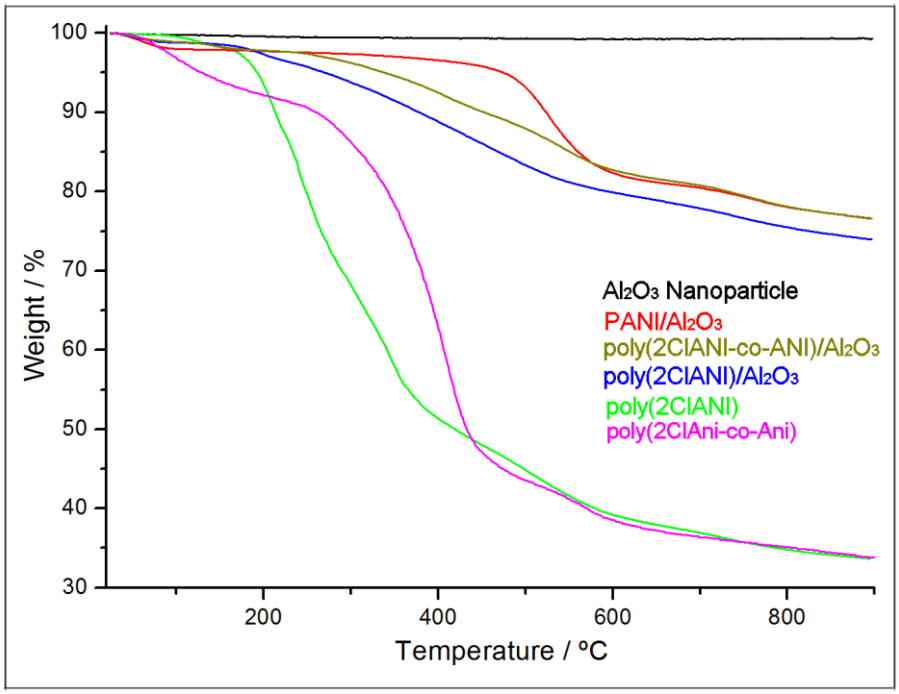

Fig. 5. Thermogravimetric analysis of poly(2ClAni), poly(2ClAni-co-Ani), Al_2O_3 nanoparticule, poly(2ClAni)/Al_2O_3, poly(2ClAni-co-Ani)/Al_2O_3 and PANI/Al_2O_3 nanocomposites obtained in nitrogen atmosphere at heating rate of 10°C/min.

The thermogram of poly(2ClAni-co-Ani) shows three distinct regions of weight loss. The initial weight loss below 120 °C (ca. 4.5 %) is attributed to the loss of water molecules. The weight loss of about 9.2 % by 240°C corresponds to the loss of acid. Beyond 240°C, the rate of decomposition is found to be maximum at 560°C and the weight loss observed is about 59.6 % wt.

The TGA curve of the poly(2ClAni)/Al_2O_3 nanocomposite also shows a weight loss between 25°C and 110°C attributed to the loss of water from both Al_2O_3 and polymer matrix. Besides a differentiated behaviour marked by a strong weight loss in the 100-450°C range is observed. Comparing poly(2ClAni)/Al_2O_3 nanocomposite with poly(2ClAni) pure; it can be seen that the incorporation of Al_2O_3 nanoparticles results in a lower weight-loss.

TGA of PANI pure showed that the first stage of weight loss occurred below 100°C, and this could be related to evaporation of water molecules from PANI. The second weight loss occurred at higher temperature, from 230 to 430°C. It was assigned to loss of dopants from PANI [40]. The third weight loss from 430°C to 640°C was due to the decomposition of PANI chains themselves.

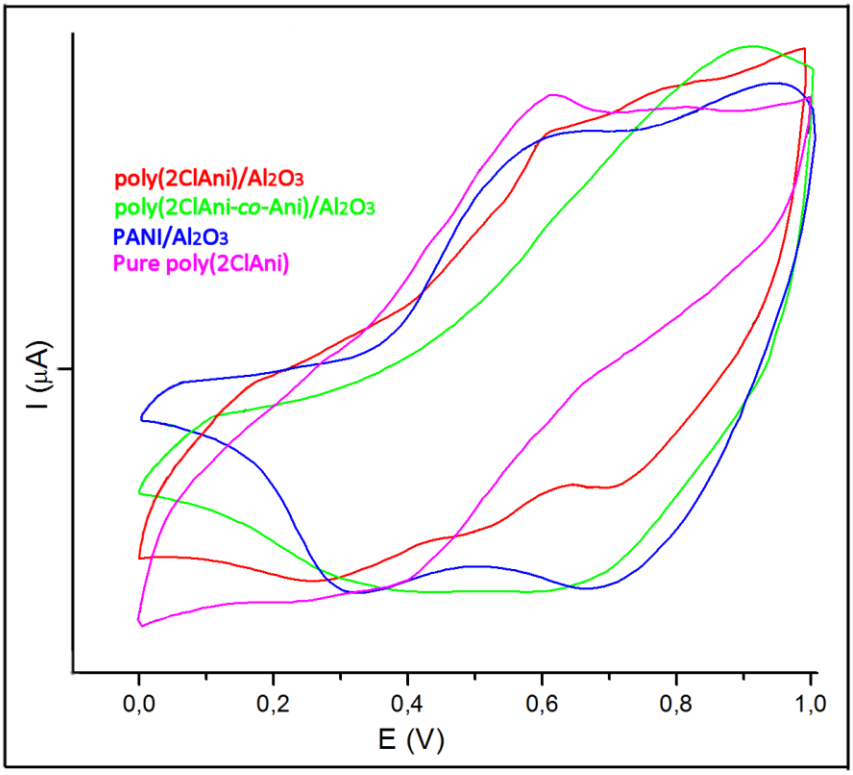

Fig. 6. Cyclic voltammograms recorded for a graphite carbon electrode covered by: poly(2ClAni) pure, poly(2ClAni)/Al_2O_3, poly(2ClAni-co-Ani)/Al_2O_3 and PANI/Al_2O_3 nanocomposites in 1M $HClO_4$ solution. Scan rate 50 mV/s.

Table 2. The electrical conductivity values of poly(2ClAni), poly(2ClAni-co-Ani), poly(2ClAni)/Al_2O_3, poly(2ClAni-co-Ani)/Al_2O_3 and PANI/Al_2O_3 nanocomposites

Samples	PANI	poly(2ClAni)	poly(2ClAni-co-ANI)	poly(2ClAni)/ Al_2O_3	poly(2ClAni-co-ANI)/ Al_2O_3	PANI/Al_2O_3
Conductivity ($S.cm^{-1}$)	$14.8x10^{-2}$	$3.89x10^{-2}$	$8.22x10^{-2}$	$2.52x10^{-3}$	$6.37x10^{-3}$	$9.21x10^{-2}$

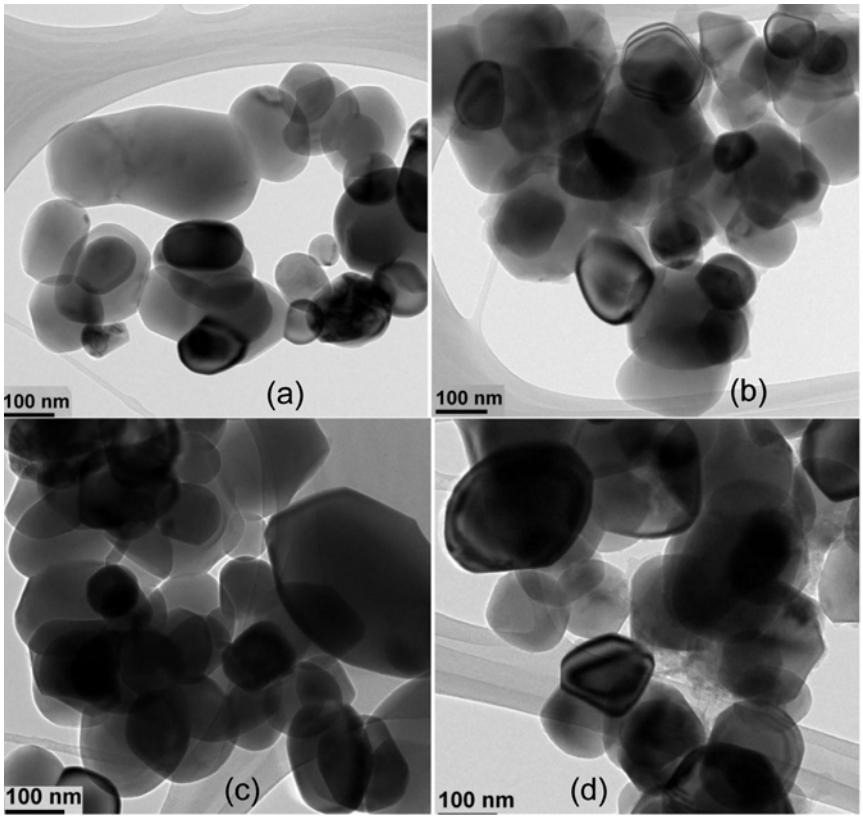

Fig. 7. TEM images of Al_2O_3 nanoparticles, poly(2ClAni)/Al_2O_3, poly(2ClAni-co-Ani)/Al_2O_3 and PANI/Al_2O_3 nanocomposites.

The TGA of PANI/Al_2O_3 nanocomposite shows three weight losses. The first decomposition step occurs from 80°C to 150°C, incurring about 2.2% weight loss, corresponding to the loss of water coming from alumina and the polymer matrix. The second weight loss occurs in the temperature range from 150°C to 500°C, which may be due, at lower temperatures to the dedoping from the polymer chain and finally to the degradation and decomposition of organic moiety and the total mass loss at up to 760˚C can be estimated to be about 23.07%. These results are similar to those obtained by Y. He [41] who found that ZnO nanoparticles improve the thermal stability of PANI to a certain extent. However; Senthilkumar et al. [42] observed that the thermal stability of PANI was relatively enhanced by forming the nanocomposites with $NiFe_2O_4$. It seems that the influence of the inorganic

nanoparticles on the thermal stability of PANI nanocomposites is very complicated; its mechanism remaining to be addressed.

On the other hand, TG of poly(2ClAni)/Al_2O_3 nanocomposite shows a 3.94% mass loss from 208 to 305˚C, which is could correspond to the dedoping from the polymer chain. After 640 ˚C, another 18.17% mass-loss is observed due to the complete degradation and decomposition of the poly(2ClAni) backbone, and the total mass loss at up to 800˚C can be estimated to be about 22.42%.

Electrochemical characterization

Cyclic voltammetry experiments were performed to test the electroactivity of the polymer and nanocomposites. Fig. 6 shows the steady-state voltammograms of poly(2ClAni) pure, poly(2ClAni)/Al_2O_3, poly(2ClAni-co-Ani)/Al_2O_3 and PANI/Al_2O_3 nanocomposites. In general, all the materials show a good voltammetric response. In particular, the observed redox processes are related to PANI-derived polymers, indicating that the polymerization on Al_2O_3 nanoparticles produces electroactive polymers. Such a good electrochemical response is in agreement with the high conductivities exhibited by the nanocomposites (Table 2). This is a very interesting result, since it demonstrates that a non-conducting material like Al_2O_3 can be successfully integrated into a conductive one by effective interaction with conductive polymers.

The addition of 2ClAni content in polymer, shows a shift of the potential peak of the redox processes associated to PANI being these redox processes less defined. It is thought that an increase in 2ClAni content in the polymer would result in a thicker coating of polymer onto Al_2O_3. Therefore, it was expected that such a thicker polymer coating could not endow effective surface area or a suitable pore structure for easy charge transfer and ion transport. In

the case of PANI/Al_2O_3, the CV presents also two overlapped redox processes. The first one appears at 0.59/0.31V, which results in a potential peak separation (ΔE_p) close to 280mV; the second process is observed at 0.94/0.67V and gives an ΔE_p value of 270mV. These redox processes are attributed to leucoemeraldine/emeraldine and emeraldine/pernigraniline transitions, respectively [43, 44]. With presence of the 2ClAni, we observe one redox peak.

Transmission Electron Microscopy

Fig. 7 depicts the TEM image of Al_2O_3 nanoparticles, poly(2ClAni)/Al_2O_3, poly(2ClAni-co-Ani)/Al_2O_3 and PANI/Al_2O_3 nanocomposites prepared by the in-situ chemical oxidative polymerization method. The Al_2O_3 nanoparticles (Fig.7a) display nearly spherical morphology and uniform particle size of ca. 100 nm diameter, similar to that observed in literature [45]. On the other hand, TEM images of nanocomposite samples show that the Al_2O_3 nanoparticles are finely dispersed into polymer matrix. This is attributed to intense turbulence and micro-mixing caused by cavitational effects due to polymerization leading to the formation of finely dispersed polymer/Al_2O_3 nanocomposites [46]. Also the particle size confirms that the composites obtained are nanostructured.

Conclusions

The polymer/Al_2O_3 nanocomposite was successfully prepared by using chemical oxidation polymerization using 2Cl-Aniline and/or Aniline monomers and Al_2O_3 in the presence of hydrochloric acid as a dopant with ammonium persulfate as oxidant. The results confirm the existence of polymer and Al_2O_3 in nanocomposites. The FT-IR studies revealed changes on the characteristic vibration bands of the polymers, confirming that they effectively interact with the surface of the Al_2O_3 nanoparticles. TGA studies revealed that the thermal stability of polymers is enhanced in the nanocomposites. The electric conductivity of the

nanocomposites has been studied. The electrochemical properties of PANI/Al_2O_3 and poly(2ClAni-co-ANI)/Al_2O_3 are better than those of poly(2ClANI)/Al_2O_3. This may be attributed to the difference in the length of the polymer chain, which results in the structural change of the polymer/Al_2O_3 interface.

Acknowledgements

This work was supported by the National Assessment and Planning Committee of the University Research (CNEPRU number E-03720130015), the Directorate General of Scientific Research and Technological Development (DGRSDT) of Algeria. The financial support from MINECO is also acknowleged (MAT2013-42007-P project).

Statement on disclosure of potential conflicts of interest

We have no conflict of interest to declare on this manuscript

References

1. S.K. Shukla, N.B. Singh, R.P. Rastogi (2013) Efficient ammonia sensing over zinc oxide/polyaniline nanocomposite. Indian Journal of Engineering & Materials Sciences. 20:319-324.

2. T.A. Skotheim, R.L. Elsenbauer, J.R. Reynold (1988) Handbook of conducting polymer, (Marcel Decker, Inc).

3. A. Mohammadi, J. Badraghi, A.B. Moghaddam, Y. Ganjkhanlou, M. Kazemzad, S. Hosseini, R. Dinarvand (2011) Synthesis of Er_2O_3 Nanoparticles and Er_2O_3 Nanoparticle/Polyaniline Deposition on the Surface of Stainless Steel by Potentiostatic Deposition. Chem. Eng. Technol. 34:56-60.

4. S.B. Kondawar, M.J. Hedau, V.A. Tabhane, S.P. Doncre, U.B. Mahatme, R.A. Mondal (2006) Studies on chemically synthesized doped poly (o-anisidine) and copoly {aniline-(o-anisidine)}. Mod. Phys. Lett. B. 23:1461-1470.

5. G. Wallace, G. Spinks, P. Teasdale (1997) Conductive electro-active polymers. Technomic Pub. Co. Inc., USA.

6. A.G. MacDiarmid (2001) A novel role for organic polymers. Synthetic metals. 125:11-22.

7. J.N. Barisci, C. Conn, G.G. Wallace (1996) Conducting polymer sensors, Trends Polym. Sci. 4:307-311.

8. D. Ghanbari, M.S. Niasari, M.G. Kooch (2016) In situ and ex situ synthesis of poly(vinyl alcohol)-Fe_3O_4 nanocomposite flame retardants. Particuology 26:87-94.

9. T.A. Vadeghani, D. Ghanbari, M.R. Mozdianfar, M.S. Niasari, S. Bagheri, K. Saberyan (2016) Sugar and Surfactant-Assisted Synthesis of $Mg(OH)_2$ Nano-flower and PVA Nanocomposites. Journal of Cluster Science. 27:299-314.

10. M.M. Arani, D. Ghanbari, M.S. Niasari, S. Bagheri (2016) Sonochemical Synthesis of Spherical Silica Nanoparticles and Polymeric Nanocomposites. Journal of Cluster Science. 27:39-53.

11. D. Ghanbari, M.S. Niasari, M.G. Kooch (2014) A sonochemical method for synthesis of Fe_3O_4 nanoparticles and thermal stable PVA-based magnetic nanocomposite Journal of Industrial and Engineering Chemistry. 20:3970–3974.

12. P. Jamshidi, D. Ghanbari, M.S. Niasari (2014) Sonochemical synthesis of $La(OH)_3$ nanoparticle and its influence on the flame retardancy of cellulose acetate nanocomposite. Journal of Industrial and Engineering Chemistry. 20:3507-3512.

13. F. Yaripour, Z. Shariatinia, S. Shariatinia, A. Irandoukht (2015) The effects of synthesis operation conditions on the properties of modified γ-alumina nanocatalysts in methanol dehydration to dimethyl ether using factorial experimental design. Fuel. 139:40-50.

14. A.A. Pechenkin, S.D. Badmaev, V.D. Belyaev (2015) Performance of bifunctional CuO-CeO_2/γ-Al_2O_3 catalyst in dimethoxymethane steam reforming to hydrogen-rich gas for fuel cell feeding. Applied Catalysis B: Environmental. 166:535-543.

15. S.Y. Hosseini, M.R.K. Nikou (2014) Investigation of different precipitating agents effects on performance of γ-Al_2O_3 nanocatalysts for methanol dehydration to dimethyl ether. Journal of Industrial and Engineering Chemistry. 20:4421-4428.

16. B.K. Sharma, N. Khare, S.K. Dhawan, H.C. Gupta (2009) Dielectric properties of nano ZnO-polyaniline composite in the microwave frequency range. Journal of Alloys and Compounds. 477:370–373.

17. D.C. Olson, J. Piris, R.T. Colins, S.E. Shaheen, D.S. Ginley (2006) Hybrid photovoltaic devices of polymer and ZnO nanofiber composites. Thin Solid Films. 496:26-29.

18. R. Sen, B. Zhao, D. Perea, M.E. Itkis, H. Hu, J. Love, E. Bekyarova, R.C. Haddon (2004) Preparation of single-walled carbon nanotube reinforced polystyrene and polyurethane nanofibers and membranes by electrospinning. Nano Lett. 4:459-464.

19. H. Yoneyama, N. Takahashi, S.Kuwabata (1992) Formation of a light image in a polyaniline film containing titanium(IV) oxide particles. J. Chem. Soc., Chem. Commun. 2:716-717.

20. A.K. Khattak, M.M. Afzal, G. Saleem, R.A. Yasmeen, R Ahmad (2000) Surface modification of alumina by metal doping Colloids Surf. A, 162:99-106.

21. B.Y. Yoo, R.K. Hendricks, M. Ozkan, N.V. Myung (2006) Three-Dimensional Alumina Nanotemplate. Electrochim. Acta. 51:3543-3550.

22. Z.Y. Wen, M.M. Wu, I. Takahito, K. Masataka, Z.X. Lin, Y. Osamu (2002) Effects of alumina whisker in (PEO)8–LiClO4-based composite polymer electrolytes. Solid State Ionics. 148:185-191.

23. C.K. Lambert, R.D. Gonzalez (1999) Sol-gel preparation and thermal stability of Pd/gamma-Al_2O_3 catalysts. J. Mater. Sci. 38:3109-3116.

24. Z. Zhang, W.H. Randall, T.R. Pauly, T.J. Pinnavaia (2002) Mesostructured forms of γ-Al_2O_3 J. Am. Chem. Soc. 124:1592-1593.

25. I. Radja, H. Djelad, E. Morallon, A. Benyoucef (2015) Characterization and electrochemical properties of conducting nanocomposites synthesized from p-anisidine and aniline with titanium carbide by chemical oxidative method. Synthetic Metals. 202:25-32.

26. Y.H. Kim, C. Foster, J. Chiang, A.J. Heeger (1988) Photoinduced localized charged excitations in polyaniline Synthetic Metals. 25:49-59.

27. M.K. Rasha (2011) Synthesis characterization, magnetic and electrical properties of the novel conductive and magnetic polyaniline/$MgFe_2O_4$ nanocomposite having the core–shell structure. Journal of Alloys and Compounds. 509:9849-9857.

28. J. Tang, X. Jing, B. Wang, F. Wang (1998) Infrared spectra of soluble polyaniline. Synthetic Metals. 24:231-238.

29. P. Linganathan, J.M. Samuel (2014) Effect of Dodecyl Benzene Sulphonic Acid on the Electrical Conductivity Behaviour of Poly(2-chloroaniline) and Poly(2-chloroaniline)/Silk Blends. American Journal of Polymer Science. 4:107-116.

30. R. S.Rengasamy, M. Jassal, C. Ramesh Kumar (2005) Studies on structure and properties of nephila-spider silk dragline. Autex Research Journal. 5:30-39.

31. P. Tarte (1967) Infrared Spectra of Inorganic Aluminates and Characteristic Vibrational Frequencies of AlO_4 Tetrahedra and AlO_6 Octahedra. Spectrochim. Acta, 23:2127-2143.

32. J. Cao, J.C. Li, L. Liu, A.J. Xie, S.K. Li, L.G. Qiu, Y.P. Yuan, Y.H. Shen (2014) One-pot synthesis of novel Fe_3O_4/Cu_2O/PANI nanocomposites as absorbents in water treatment. J. Mater. Chem. A. 2:7953-7979.

33. D.A. Seanor (1982) Electrical Properties of Polymers, Academic Press, New York pp 2-3.

34. B. Sari, M. Talu (1998) Electrochemical Polymerization and Analysis of Some Aniline Derivatives. Turkish Journal of Chemistry. 22:301-307.

35. J.M. Ginder, A.J. Epstein (1990) Role of ring torsion angle in polyaniline: Electronic structure and defect states. Physical Review B. 41:10674,

36. J. Arias-Pardilla, H.J. Salavagione, C. Barbero, E. Morallón, J.L. Vázquez (2006) Study of the chemical copolymerization of 2-aminoterephthalic acid and aniline.: Synthesis and copolymer properties. European Polymer Journal. 42:1521-1532.

37. Pavel Afanasiev (2015) Non-aqueous preparation of $LaPO_4$ nanoparticles and their application for ethanol dehydration. RSC Advances. 5:42448-42454.

38. S. Bitao, M. Shixiong, S. Shixiong, T. Yongchun, B. Jie (2007) Synthesis and characterization of conductive polyaniline/TiO_2 composite nanofibers. Front Chem China. 2:123-126.

39. Y. Wei, G. W. Jang, K. F. Hsueh, A. G. MacDiarmid, A. J. Epstein (1992) Thermal transitions and mechanical properties of films of chemically prepared polyaniline. Polymer. 33:314- 322.

40. S. Shahabuddin, N.M. Sarih, F.H. Ismail, M.M. Shahid, N.M. Huang (2015) Synthesis of chitosan grafted-polyaniline/Co_3O_4 nanocube nanocomposites and their photocatalytic activity toward methylene blue dye degradation. RSC Advances. 5:83857-83867.

41. Y. He (2004) Preparation of polyaniline/nano-ZnO composites via a novel Pickering emulsion route. Powder Technology. 147:59-63.

42. B. Senthilkumar, K.V. Sankar, C. Sanjeeviraja, R.K. Selvan (2013) Synthesis and physico-chemical property evaluation of PANI–$NiFe_2O_4$ nanocomposite as electrodes for supercapacitors. Journal of Alloys and Compounds. 553:350–357.

43. K.S. Ho, T.H. Hsieh, C.W. Kuo, S.W. Lee, J.J. Lin, Y.J. Huang (2005) J. Polym. Sci., Part A: Polym. Chem., 43:3116.

44. S. Cho, J.S. Lee, J. Jun, J. Jang (2014) High-sensitivity hydrogen gas sensors based on Pd decorated nanoporous poly(aniline-co-aniline-2-sulfonic acid):poly(4-styrenesulfonic acid). Journal of Materials Chemistry A. 2:1955.

45. M. Goudarzi, D. Ghanbari, M.S. Niasari, A. Ahmadi (2016) Synthesis and Characterization of $Al(OH)_3$, Al_2O_3 Nanoparticles and Polymeric Nanocomposites. Journal of Cluster Science. 27:25-38.

46. A. Bhanvase, S.D. Kamath, U.P. Patil, H.A. Patil, A.B. Pandit, S.H. Sonawane (2016) Intensification of heat transfer using PANI nanoparticles and PANI-CuO nanocomposite based nanofluids. Chemical Engineering and Processing. 104:172-180.